Computer-assisted Diagnosis of CT Pulmonary Images

Dr Alan C Horwood BA, PhD (A.C.Horwood@Bristol.ac.uk) Tel. +44 (0)117 9743

Professor S J Hogan MA, PhD

Professor P R Goddard BSc, MD

Dr Jonathan Rossiter PhD

Department of Engineering Maths, University of Bristol, Clifton, Bristol BS8 1TR, UK.

May 2001

Purpose: to produce a robust algorithm as the basis of a computer program for diagnosing pulmonary images from computed tomography (CT) scans.

Materials and Methods: single slices are extracted from complete CT data-sets and normalized for radio-density / greyscale relationship. Normalization is discussed in a companion paper; it is an essential image pre-processing procedure. Modal greyscale values in regions of the parenchyma provide indices of physiological or pathological conditions. The application of thresholds focuses attention around three characteristic values that correspond to below-normal, normal and above-normal tissue densities for given locations. Plots of the thresholded pixels form patterns that map the corresponding range of densities; their number and distribution characteristics – assessed using information dimensions – providing the diagnostic criteria. Parameters are empirically derived by analysis of a variety of data-sets.

Results: an algorithm using pixel counts and information dimensions of patterns derived from standard greyscale thresholds gives consistent and reliable diagnoses for all slices within the training sets: 97% accuracy, 100% sensitivity and 96% specificity.

Conclusion: a promising approach to the task of formulating computer-based automatic, or semi-automatic diagnosis of the lungs, uses algorithms based on quantifying the pixel plots that result from appropriate greyscale thresholding. The method may prove applicable to other organs that have a fractal-like structure.

Computer-assisted Diagnosis of CT Pulmonary Images

INTRODUCTION

The fractal structure of the broncho-vascular tree results from the nature of lung morphology. [1,2,3,4,5,6] It provides an efficient network for transporting air and blood to the alveoli and accounts for the fairly homogeneous tissue density across the lung parenchyma. [7] In CT scans, local density is recorded as the reduction in x-ray intensity per unit thickness of material, using the arbitrarily defined Hounsfield scale. Air and water are assigned attenuation values of –1000 Hu and 0 Hu respectively, giving bone a range of values from around +80 Hu to +1000 Hu and beyond. Local parenchymal density is decreased by lesions occurring as residual air pockets beyond the terminal bronchioles, and increased by fibrotic scarring. In CT images, density data are reconstructed using a greyscale contrast range of 0 (black) to 255 (white). The image pixels are points of varying brightness that depend directly on the x-ray attenuation coefficients. Where attenuation values deviate from the normal range for the particular tissue, there will be darker or lighter than normal greyscale levels in the corresponding images. The sensitivity of CT to parenchymal density changes makes such deviations from ‘normal’ greyscale values good indices of disease. [8]

Computer analysis of a medical image based on densitometry depends crucially on the recognition of a specific range within the greyscale distribution that is indicative of a particular physical condition. [9] Especially important is the modal value representing ‘normal’ in a given thoracic location, appropriate for the patient’s posture during scanning. Pixels within and close to the modal range for ‘normal’ can be segmented as a pattern for assessment in terms of quantity and distribution of points and compared with

empirically derived parameters for health. In defining such criteria, one must take account of complicating factors responsible for possible irregularities in reconstructed image slices. CT scans are usually (though not always) taken with the patient supine, which means that, among other things, varying effects of pressure and gravity on organs such as the lungs must be taken into account. Differences in patients' size and weight affect image quality. [10] There is always some density gradient from anterior to posterior, though the observed greyscale shift across data-sets ranges from 5 to 13 points in the original, unprocessed images. Other complicating factors include the use of a contrast medium, variable scanning parameters of range and level and impulsive noise. [11]

MATERIALS AND METHODS

Regions of interest ('roi's')

For purposes of learning and training, 50x50 image regions that are known to contain a significant number of pixels representing lower-than-normal, normal, or higher-than-normal tissue density are selected from a number of CT data-sets. From each of these images, three pixel patterns (plots) are segmented using empirically derived upper and lower threshold values to contain, respectively, the characteristic density-related greyscale distribution ranges. A histogram of the greyscale distribution in the pixel plot reveals its mode(s). However, as already suggested, though one expects a low-deviation modal greyscale distribution in images of most lesion-free parenchyma – certainly in the lung fields – the actual mode value is not guaranteed to be the same from one data-set to another, even for similar locations. The term 'normalization' refers to image pre-processing designed to correct such differences by shifting the relative brightness values up or down, using a standardized 'normal' value as a reference. [11]

The segmented regions of interest from normalized data-sets can be assessed for their relative distributions of pixels falling within standardized threshold 'windows'. With a normalized greyscale mode of 35 (approximately corresponding to –722Hu) taken to signify a healthy anterior region, a plot of pixels from within the range 30 to 40 should comprise almost all pixels corresponding to 'normal' density. However, further image processing will change the actual greyscale values employed. (See below) The 50x50 format means that, in an image region comprising only the parenchyma, the expected number of pixels will be close to 2000. Pixels representing abnormal densities will be excluded by this 'window' and will need to be registered by two further windows, one thresholded to 'see' the lower than normal greyscale values, the other only the higher ones. The distribution of pixels within a plot can be assessed by estimating the fractal dimension. [9] A distribution comprising pixels of near-homogeneous greyscale values will have a fractal dimension around 1.90. [11] The diagnostic interpretation of assessed values depends on clinical judgment.

Greyscale parameters

Information dimension is used as a fractal estimator in preference to the more usual capacity dimension, because it is more sensitive to the pattern of pixel distribution in thresholded images. [9] The 50x50 regions of interest, with pixel greyscale distributions characterizing regions of known normal or pathological condition, are used in devising a diagnostic algorithm. They are selected anteriorly and posteriorly from image slices taken from eight data-sets. Each slice is in a 512x512 format, individually selected from complete image scans produced using a Siemens Somaton Plus 4 whole-body spiral scanner.

Trials extend over a large number of samples from the data-sets, though the methodology can be demonstrated using one slice. Set 2 has a slice at anatomical level around T6/7 that shows each of the three types of tissue under test: normal, emphysematous and fibrotic. Sampling the visually normal anterior region shows a modal greyscale value of 11. For normalization purposes, a correlation has been established between the soft tissue mode characterizing the set and the % brightness increase needed to set the normal anterior value to 35. [11] In this data-set, the soft tissue mode is 82, a value shown empirically to indicate a brightness increase of 9.8% – in practice, 10%, for normalization. When this increase is applied, the anterior greyscale mode does indeed move from 11 to 35 and, importantly, without change of the distribution profile. A further, advisable, step in the pre-processing is a small degree of smoothing to remove any impulsive noise. A 3x3 mask is used to apply the average neighbourhood greyscale value to the central pixel. The modal value of the distribution remains unchanged.

When 50x50 regions showing, respectively, emphysema and fibrosis are selected from the normalized slice, the greyscale ranges representing the two abnormal conditions can be established. From these results, the thresholds for the diagnostic ‘windows’ can be determined. When the results from this and a wide range of other slices are correlated, typical diagnostic modal greyscale values for the three broad types of anterior and posterior (or gravity-dependent) tissue are as those set out in table 1.

Table 1: typical modal greyscale values for images of various tissue conditions in anterior and posterior regions

	Anterior region	Posterior region
Normal parenchyma	**35**	**45**
Emphysematous tissue	**23**	**26**
Fibrotic tissue	**70**	**75**

A second phase of image processing is designed to extend the working range over a greater part of the whole grey scale. Among other things, this allows a clearer separation between the normal and abnormal distributions. The simple technique is an application of a so-called image arithmetic algorithm which, in effect, multiplies individual pixel values by a given factor. Pixels corresponding to the chest wall, hilum and mediastinum acquire a range of greyscale values from c.220 to 255, and are easily excluded from the upper diagnostic window. In these tests, a factor of 2 is used. The modified modes appear in table 2.

Table 2: typical modal greyscale values for images of various tissue conditions in anterior and posterior regions, modified after pixel values are enhanced by x2

	Anterior region	Posterior region
Normal parenchyma	**70**	**90**
Emphysematous tissue	**45**	**50**
Fibrotic tissue	**140**	**155**

These values suggest possible diagnostic thresholds for the anterior regions of 40 – 55, 55 – 110 and 130 – 170, with 40 – 65, 75 – 120 and 130 – 170 for the posterior.

Diagnostic filters

The three pairs of threshold ranges act as greyscale filters that isolate those pixels found empirically to represent ‘below normal’, ‘normal’ and ‘above normal’ parenchymal densities in anterior and posterior regions of the lung fields. When these

filters are applied to standardized image regions, the resultant pixel patterns have distributions that characterize particular conditions of the parenchyma. Both the number of pixels isolated and their space-filling character are important indices.

By whatever means they are selected, the 50x50 regions will comprise pixels that correspond either entirely to lung tissue, or only partially so, with others representing an area of chest wall, mediastinum etc. Application of the three types of window should distinguish between the latter case and a situation where the 'missing' pixels represent a diseased state: in the former, no pixel pattern will emerge in the 'high' range; but in the latter, there will be at least one distribution of 'abnormal' pixels either in the 'low', or 'high' range – or in both.

Illustrated application

The 50x50 images selected from the processed slice represent three regions of parenchyma: the right anterior, 'a', right posterior, 'b' and left posterior,'c'.

Fig. 1: three regions from slice 33 of data-set 2, representing normal, fibrotic and emphysematous tissue, with corresponding thresholded pixel plots

(a) **(b)** **(c)**

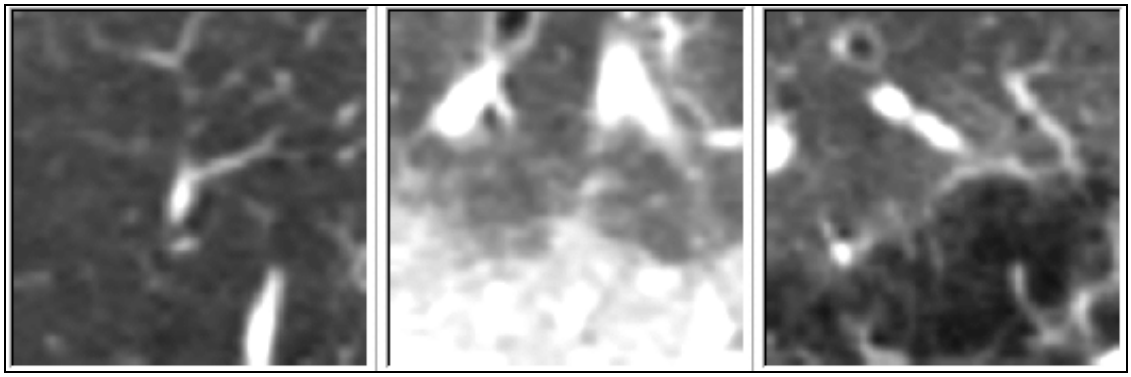

Applying the appropriate 'diagnostic' threshold filters to each of the three images results in the following pixel plots: figures 2a, 2b and 2c.

Fig. 2a: pixel distribution using the appropriate 'low' window

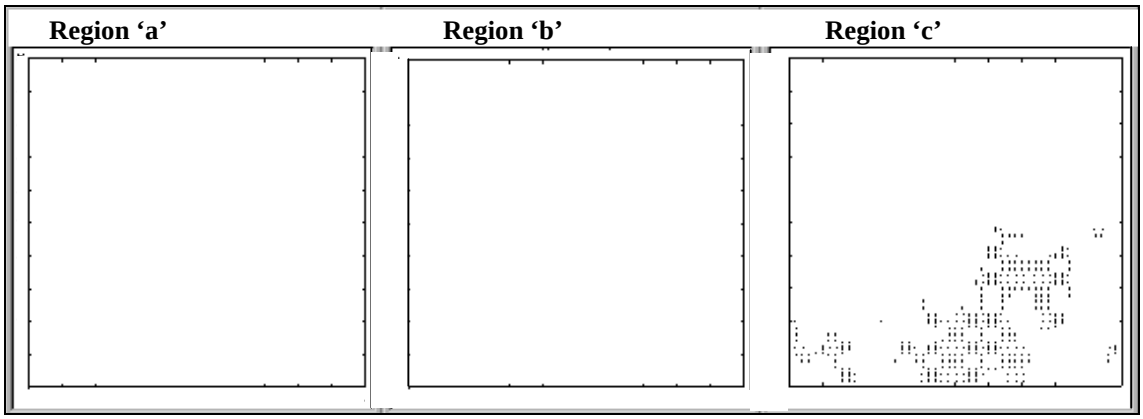

Pixel count: no. of pixels representing below-normal densities in the three regions

selected pixel range:	40 to 55	selected pixel range:	40 to 60	selected pixel range:	40 to 65
pixels below selected range:	1	pixels below selected range:	0	pixels below selected range:	0
pixels above selected range:	2499	pixels above selected range:	2500	pixels above selected range:	2129
pixels inside selected range:	0	pixels inside selected range:	0	pixels inside selected range:	371

Assigned information dimensions: region 'a' —; region 'b' —; region 'c' 1.57

Fig. 2b: pixel distribution using the appropriate 'normal' window

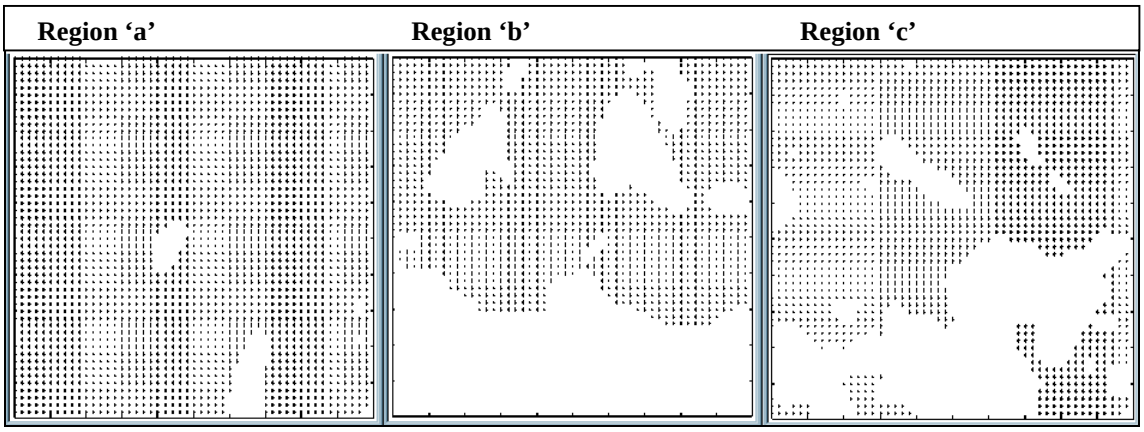

Pixel count: no. of pixels representing normal densities in the three regions

selected pixel range:	55 to 110	selected pixel range:	75 to 120	selected pixel range:	75 to 120
pixels below selected range:	1	pixels below selected range:	11	pixels below selected range:	687
pixels above selected range:	71	pixels above selected range:	1097	pixels above selected range:	108
pixels inside selected range:	2428	pixels inside selected range:	1392	pixels inside selected range:	1705

Assigned information dimensions: region 'a' 1.94; region 'b' 1.80; region 'c' 1.84

Fig. 2c: pixel distribution using the appropriate 'high' window

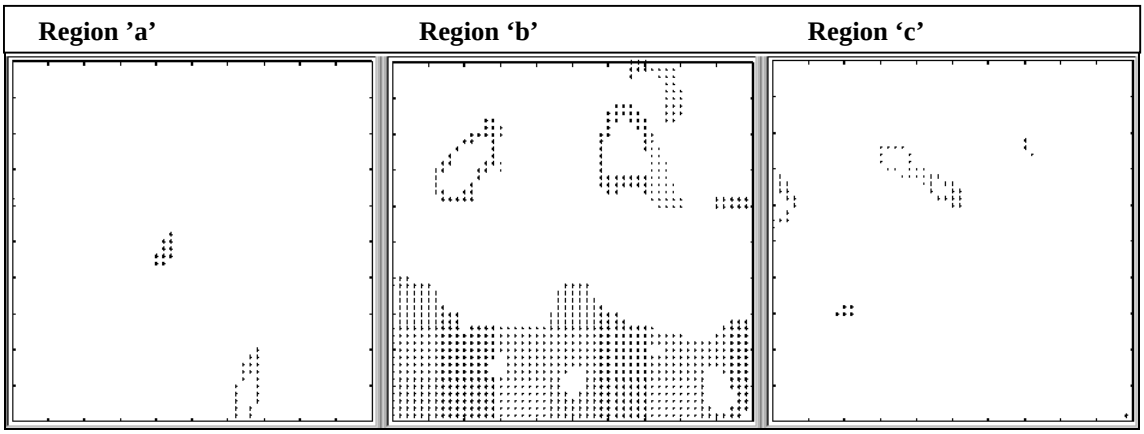

Pixel count: no. of pixels representing above-normal densities in the three regions

selected pixel range:	130 to 170	selected pixel range:	130 to 170	selected pixel range:	130 to 170
pixels below selected range:	2460	pixels below selected range:	1543	pixels below selected range:	2426
pixels above selected range:	9	pixels above selected range:	100	pixels above selected range:	18
pixels inside selected range:	31	pixels inside selected range:	857	pixels inside selected range:	56

Assigned information dimensions: region 'a' 0.96 ; region 'b' 1.77; region 'c' 1.03

Interpreting results

As already suggested, a 50x50 image of normal, peripheral, lung parenchyma should contain very few pixels in plots generated using the 'low' or 'high' diagnostic windows: too few to produce an information dimension of a significant value. Just what is to count as 'significant' is dependent on correlating assigned values with clinical diagnoses. Region 'a' in the illustrated example is clearly a case of lesion-free parenchyma: there are 2428 pixels in the normal range, 0 in the 'low' range, and 31 in the 'high'. This last number registers the few higher densities due to large vessels and, possibly, structural elements such as septa. The information dimension for the 'normal' plot is 1.94, which meets the criterion of 'a distribution comprising pixels of near-homogeneous greyscale values having a fractal dimension around 1.90.'[11] The clearly

visible patch of emphysema in region ‘c’ has an estimated information dimension of 1.57 which, therefore, must be taken as meeting a criterion value for this condition. Region ‘b’ has 857 ‘high-value’ pixels, whose plot has an estimated information dimension of 1.77. These figures are clear indices of the visible fibrosis. Wherever an abnormal patch is registered, the information dimension, using the ‘normal’ window, will be < 1.85.

Tests on regions of known clinical condition, from eight data-sets

An extension of the application to test slices taken from eight data-sets yields the results summarized in table 3. A heuristic criterion, based on the foregoing, is used to indicate the diagnostic implication of the pixel distribution: an information dimension < 1.90 for a plot of ‘normal’ pixels is taken as a sign of possible abnormality. This requires an investigation of values registered in the lower and higher windows to see whether emphysema or fibrosis may be expected. When these windows are used, dimensions > 1.30 and 1.40 are taken, respectively, as significant values.

Table 3: summary of results for test slices, one from each data-set

		Comment
Number of data-sets	**8**	**one slice selected from each**
Number of regions tested	**24**	**in each case, ‘a’, ‘b’ & ‘c’**
Number indicated ‘normal’	**16**	**visually confirmed correct**
Number indicated ‘possibly emphysematous’	**2**	**set 2, slice 33, region ‘c’ (c)** **set 7, slice 24, region ‘b’ (fp)**
Number indicated ‘possibly fibrotic’or ‘opacified’	**6**	**set 2, slice 33, region ‘b’ (c)** **set 4, slice 10, regions ‘b’ & ‘c’ (c)** **set 5, slice 6, region ‘b’ (c)** **set 8, slice 30, region ‘a’ (c)**
Number not classified	**1**	**set 6, slice 15, region ‘b’ (?)**

Key: (c) means correctly identified, (fp) false positive, (?) no diagnosis returned

The physiological condition of the chosen regions was, in each case, previously known. They serve as a ‘training’ set to ‘fine tune’ the diagnostic parameters. In these returns there are no false negatives, one false positive and one not classified. The false positive resulted from a slightly over-large allowance for gravity-dependence in region ‘b’. The patient scanned to produce data-set 7 was, in fact, quite thin and lightweight. Weight is one of the factors responsible for irregularities in CT images. Fine-tuning the thresholding parameters for the ‘normal’ posterior window corrected the diagnostic readout; the diagnoses remained correct for all other slices when the modified window was used. The change is from 75 – 120 to 72 – 120.

The one region unclassified returned a count of 1577 pixels in the ‘normal’ window, with an information dimension of 1.89; only 108 pixels showed up in the ‘high’ window, information dimension 1.28, but 694 were found in the range 200 – 255, information dimension 1.91. Such a compact mass suggests one of two possibilities: either a non-parenchyma region in the image, or a large metastatic deposit. Nodules have densities very similar to soft tissue or end-on blood vessels, so cannot be distinguished easily using densitometry. In the case of the unclassified region, the somewhat lower density ring around a large nodule was registered in the ‘high’ window, but the large mass was outside the threshold range. The plots are shown in figure 3.

Fig. 3: the unclassified region seen through the 'normal', 'high', and top range windows

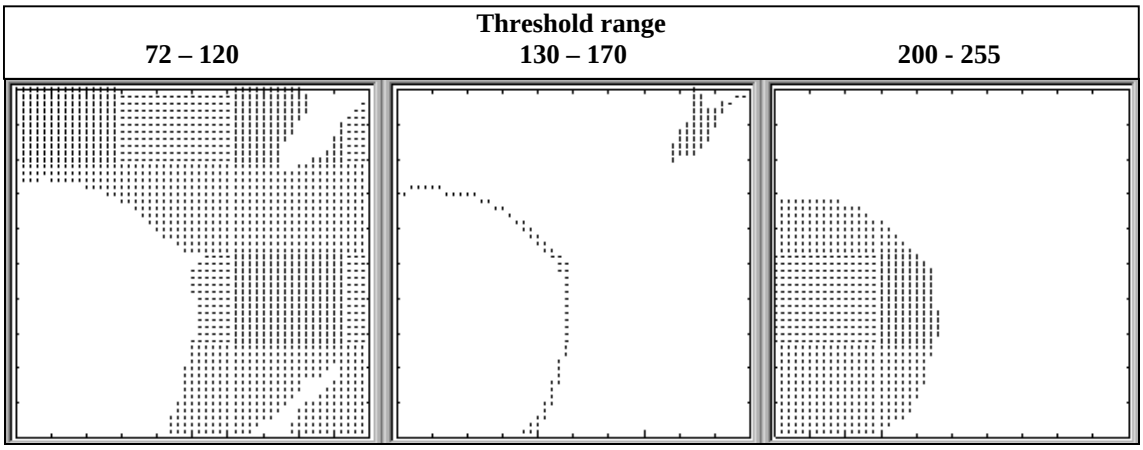

A check for any distribution within the 200 to 255 range helps identify the character of the tissue corresponding to the 'missing' pixels. The diagnosis is by inspection.

Extension of the tests to all slices in the data-sets, 442 in total, produced the results summarized in table 4.

Table 4: performance assessment

True positives	**119**	**accuracy (freedom from mistake):**	**97%**
True negatives	**310**	**sensitivity (ability to diagnose abnormality)**	**100%**
False positives	**13**	**specificity (correct diagnosis of normality)**	**96%**
False negatives	**0**		

NB: Data used in the estimation of diagnostic accuracy are from the data-sets used to create the diagnostic algorithm. As such, the performance assessment is merely an indication of the consistency of the application. Nevertheless, this is important. Results compare favourably with those quoted for other studies, such as the use of multiple features in texture-based tissue characterization [12]

Selecting regions for examination

A processed image slice comprises pixels from almost the complete greyscale range. The meaning of a particular aggregation of pixels is clear to one with experience of medical image interpretation, but makes sense to a computer only when a range of thresholded greyscale values is segmented and given a label. Regions of interest are those containing pixels corresponding to the lung parenchyma. With the normalization

and standard processing adopted for this study, all corresponding greyscale values will lie between 40 and 170. The pixel plots resulting from the segmentation imposed by the threshold limits of the diagnostic windows will map various conditions of the parenchyma. How might the appropriate regions be selected?

So far in this demonstration, 50x50 regions have been selected by inspection. In an automatic (or semi-automatic) application, a quicker, more independent process is needed. For satisfactory diagnoses, all parts of the parenchyma must be divided into somewhat smaller regions to give an optimum cover. Figure 4 illustrates a possible way of selecting and identifying regions of interest using a labelled grid. Each square measures 32x32 pixels. Only regions containing pixels within the greyscale limits 40 and 170 (inclusive) are selected for assessment.

Note: in the figure, the image region beyond the chest wall contains greyscale values similar to the emphysematous patch at the left posterior; regions are not selected from beyond the boundary of the thorax. The computer can be programmed to recognize the closed boundary of the chest wall, and ignore all pixels from outside. The chest wall itself will have no pixels with greyscale values <180, so will not contribute to the pixel count established by the ‘high’ diagnostic window.

Fig. 4: a grid for selecting regions of interest from a tomographic pulmonary slice

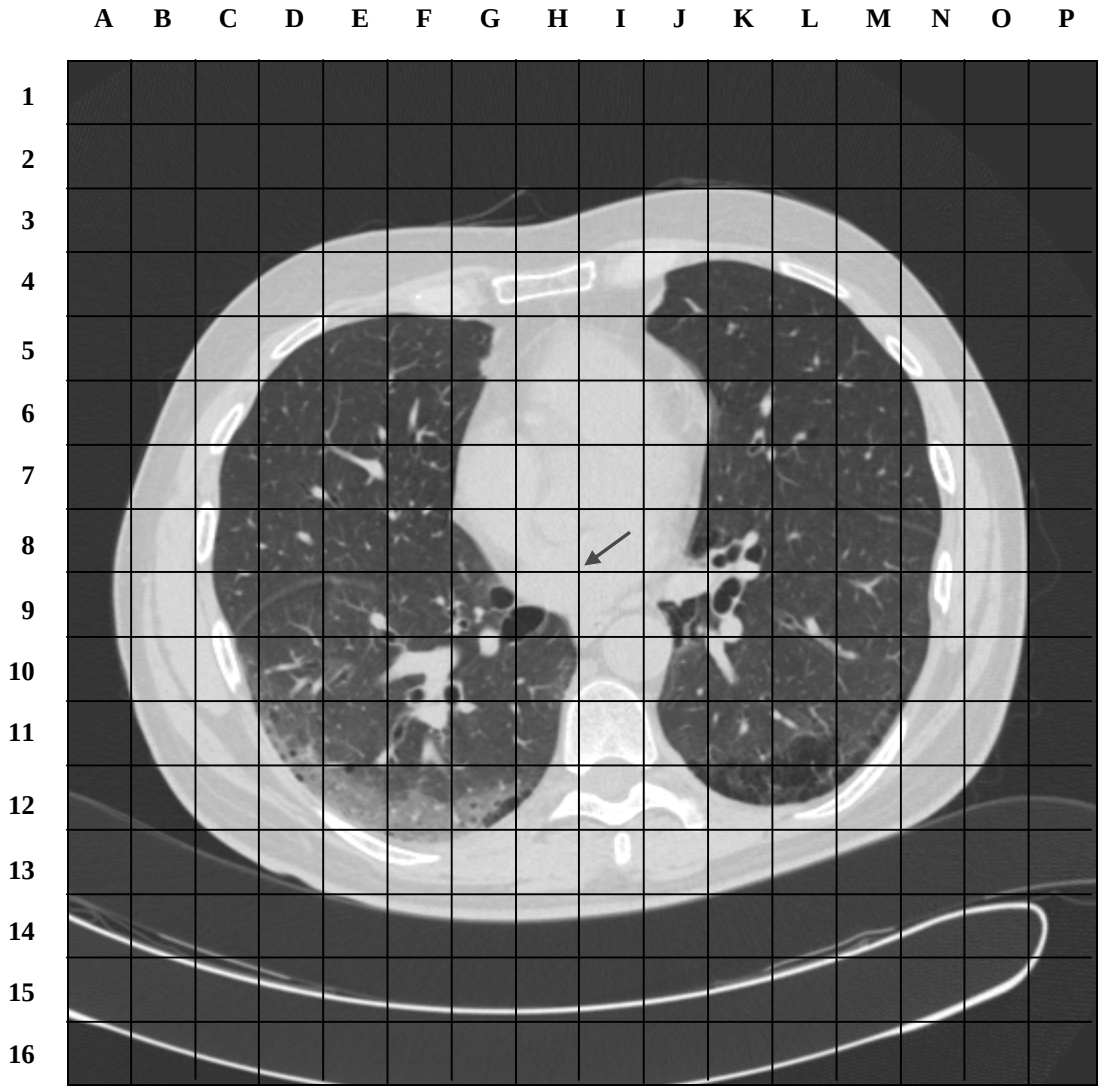

The centre of the grid, marked with an arrow, is at the centre of the image; the boxes selected as regions of interest are identified using the grid references. In this case, the regions selected are 4J, 4K, 4L, 5D, 5E, 5F, 5G, 5J, 5K .....12D, 12E, 12F, 12G, 12H, 12J, 12K, 12L, 12M & 13F, using the stated criteria. Where tests suggest abnormality, adjacent slices must be inspected to see whether there is an appropriate continuity of the feature.

An inspection of the lung image immediately discloses the problem of distinguishing between those low-value greyscale pixels representing emphysema and those that correspond to cross-sections of bronchi: each are in the range 48 to 70, so will register in the 'low' windows. Two additional features may be useful for diagnosis. An emphysematous bulla will be in the same position across several adjacent slices, whereas bronchi will usually 'travel' obliquely. A patch of emphysematous tissue will have a rough boundary; a bronchus will not. An application of the Hough transform should help identify the object with the more regularly curved border. [13] Ultimately, the decision rests on inspection by a trained eye.

A diagnostic algorithm

Figure 5 sets out a prototype for a diagnostic algorithm needed as the basis of projected computer software. Robustness is essential, though such an algorithm is inevitably heuristic, since 'health' and 'abnormality' are rather fuzzy concepts – especially as expressed through image functions. Implicit in their use are working definitions of what signifies tissue abnormality in the structures and patterns of image features. In the diagnosis of CT images, the underlying feature is density: implications for health suggested by particular patterns of tissue radio-density are assessed using the corresponding greyscale values in aggregations of pixels. 'Low', 'normal' and 'high', as applied to threshold limits, are imprecise categories: there are overlapping, shadowy regions at the boundaries. We are looking along a 'health' spectrum and assigning boundaries between degrees of what is 'acceptable' and what should cause concern, without ever being able to say precisely when 'rudely healthy' becomes 'not quite right'. Ultimately, judgements depend on a trained clinician arbitrarily assigning degrees of significance to characteristic signs in the pixel patterns.

Fig. 5: a diagnostic algorithm for assessing 32x32 pixel regions in CT pulmonary images

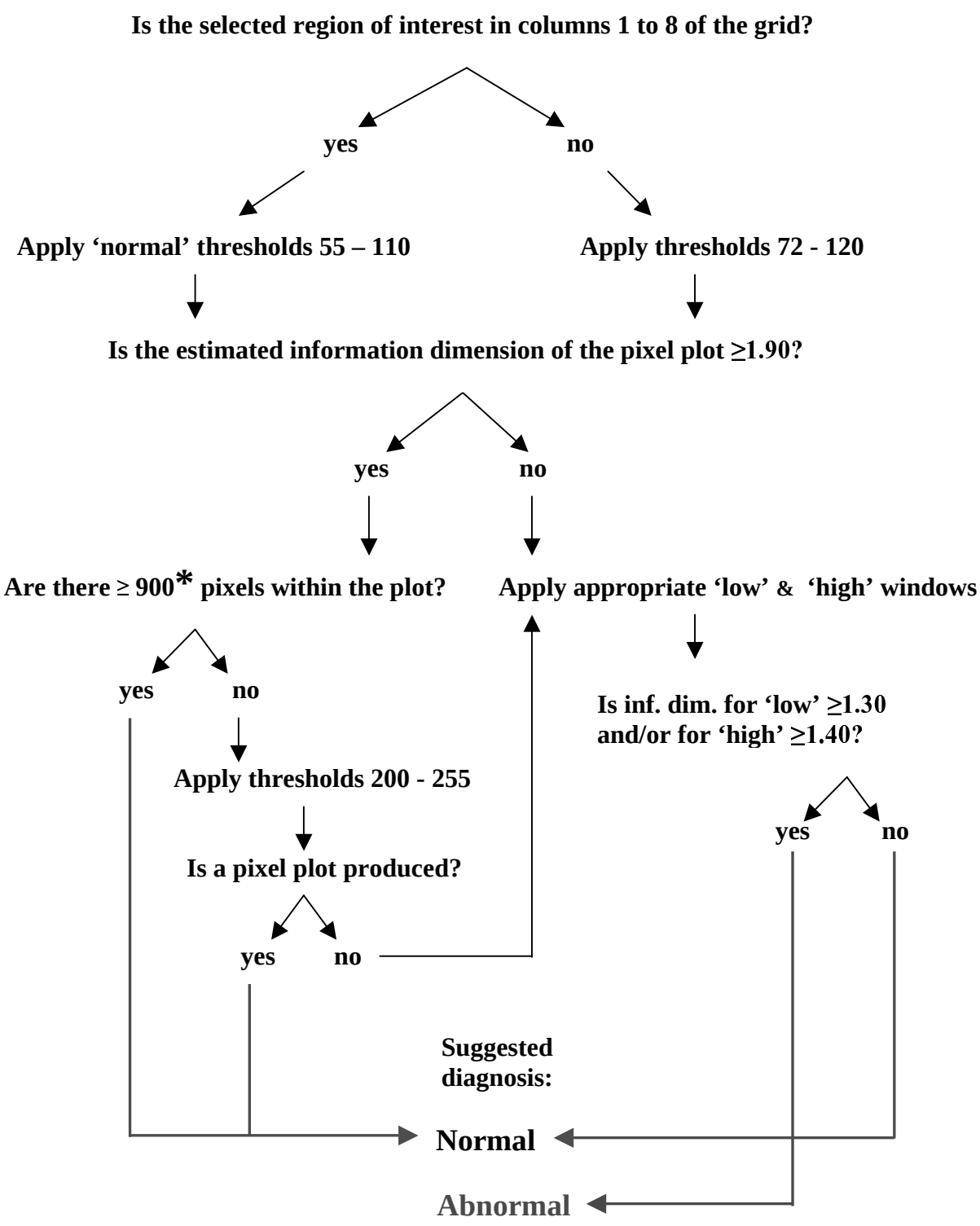

* **NB: 900 for a 32x32 plot, 2100 for 50x50**

DISCUSSION

A series of diagnoses of medical image showing no false negatives and a 97% freedom from all errors is encouraging. The empirically derived algorithm is simple enough to use as the basis for a trial version of diagnostic computer software. Application of such a program can run parallel with the manual procedures outlined above and comparisons made over a large number of CT lung data-sets.

An instruction to inspect slices adjacent to that where abnormality is suspected might have been included as a further step in the algorithm, though this operation is best carried out by the clinician since visual confirmation of a signalled abnormality is essential. Looked for, is the continuity of a feature consistent with its size. For instance, some evidence of a patch of emphysema of width, say, 100 pixels, in a slice from a spiral scan with a typical collimation of 2 or 3 mm, would be expected to show up in at least four other neighbouring slices and, importantly, with similar spatial coordinates.

The grid itself, while primarily a device for identifying and selecting regions of interest, can be programmed to apply the appropriate diagnostic windows and feed data to the algorithm. In its simple form, the algorithm is equipped to deal with either anterior or posterior regions, defined as above or below the central horizontal grid line. In a more sophisticated form, each row of the grid might have its own set of thresholding parameters, corresponding to the continuous density gradient from non-dependent to dependent regions.

Consistency of results is contingent on satisfactory normalization of the images. The crucial condition is the close match across all data-sets of the modal greyscale value for normal parenchyma in similar locations. A safe judgment on the reliability of diagnoses will need extended trials. The aim of this paper is to outline a methodology and suggest

a means of implementation. The results for the eight data-sets from which the various parameters have been derived are quite consistent and, therefore, encouraging.

Although attention has been exclusively directed towards CT pulmonary images, any organs with a fractal structure – kidneys, for example – might produce images suitable for a modified form of this application. [14,15,16,17]

REFERENCES

1 Tsonis A. & Tsonis P. Fractals: a New Look at Biological Shape and Patterning. Perspectives in Biology and Medicine, vol. 30 no. 3. Spring 1987. pp. 355-361.

2 Weibel E R. Design of airways and blood vessels considered as branching trees. In 'The Lung: Scientific Foundations' (edited various); NY. Raven, 1991, pp. 711-720.

3 Weibel E R. Fractal geometry: a design principle for living organisms. (American Physiological Society.) Am. J. Physiol. 1991 no. 261, pp. L361-L369.

4 Krenz G, Linehan J, Dawson A. A Fractal Continuum Model of the Pulmonary Arterial Tree. J. Appl. Physiol. vol.72 no. 6, 1992. pp. 2225-2237.

5 Albertine K. Structural Organization and Quantitative Morphology of the Lung. Chapter 4: Application of Magnetic Resonance to the Study of Lung, ed. Cutillo, Armonk, NY. Futura Publishing co. Inc. (c) 1996.

6 Huang W, Yen R, McLaurine M, Bledsoe G. Morphometry of the Pulmonary Vasculature. J. Appl. Physiol. vol. 81 no. 5, 1996. pp. 2123-2133.

7 West G. B, Brown J, Enquist B. A General Model for the Origin of Allometric Scaling Laws in Biology. SCIENCE, vol. 276, 4 April 1997. pp. 122-126; reviewed in The Guardian of April 17, 1997.

8 Hartley P, Galvin J, Hunninghake G, Merchant J, et al. High-resolution CT-derived measures of lung density are valid indexes of interstitial lung disease. J. Appl. Physiol. 1994 no. 76(1), pp. 271-277.

9 Horwood A. Computer Diagnosis of Tomographic Pulmonary Images. Bristol, PhD Dissertation, 2000.

10 Huda W, Scalzetti E, Levin G. Technique Factors and Image Quality as Functions of Patient Weight at Abdominal CT. Radiology Nov 2000; 217 (2), pp 430-435.

11 Horwood A, Hogan S J, Goddard P, Rossiter J. Image Normalization, a Basic Requirement for Computer-based Automatic Diagnostic Applications. Submitted to Radiology as a companion paper.

12 Uppaluri R, McLennan G, Sonka M, Hoffman E. Computer-based objective quantitative assessment of pulmonary parenchyma via X-ray CT. http://everest.radiology.uiowa.edu/spie/spie98/re1/SPIE98.html

13 Sonka M, Hlavac V, Boyle R. Image Processing, Analysis and Machine Vision. pp. 149-161 First printed by Chapman & Hall, 1993, reprinted by International Thomson Computer Press, London 1996. ISBN 0-412-45570-6

14 Caldwell C, Stapleton S, Holdsworth D, Jong R, Weiser W, et al. Characterization of Mammographic Parenchymal Pattern by Fractal Dimension. Phys. Med. Biol. 1990 vol. 35. pp. 235-247

15 Mainster M. The Fractal Properties of Retinal Vessels: Embriological and Classical Implications. Eye no.4, 1990. pp. 235-41.

16 Cross S, Start R, Stephenson T, Cotton D. Fractal Geometric Analysis of the Renal Arterial Tree in Infants and Fetuses. Pediatric Pathology & Laboratory Medicine no. 15,1995. pp.259-268.

17 Priebe C, Solka J, Lorey R, Rogers G, Poston W, et al. The application of fractal analysis to mammographic tissue classification. Cancer Letters no. 77, 1994. pp. 183-189.